International Journal of Biological Macromolecules 296 (2025) 139630

Contents lists available at ScienceDirect

International Journal of Biological Macromolecules

journal homepage: www.elsevier.com/locate/ijbiomac

Exploring *in vitro* efficacy of rCHAPk with antibiotic combinations, and promising findings of its therapeutic potential for clinical-originated MRSA wound infection

Semra Tasdurmazli [a], Irfan Cinar [b], Murat Karamese [c], Selina Aksak Karamese [c], Elif Cadirci [d], Luís D.R. Melo [e,f,g], Tulin Ozbek [a,*]

[a] Yıldız Technical University, Faculty of Science and Arts, Department of Molecular Biology and Genetics, Istanbul, Turkey
[b] Kastamonu University, Faculty of Medicine, Kastamonu, Turkey
[c] Kafkas University, Faculty of Medicine, Kars, Turkey
[d] Ataturk University, Faculty of Medicine, Erzurum, Turkey
[e] Center of Biological Engineering, University of Minho, 4710-057 Braga, Portugal
[f] LABBELS –Associate Laboratory, Braga, Guimarães, Portugal
[g] Faculty of Pharmacy, University of Coimbra, 3000-548 Coimbra, Portugal

ARTICLE INFO

Keywords:
Endolysin rCHAPk
Endolysin-antibiotic synergism
MRSA-infected *in vivo* wound model

ABSTRACT

The increasing threat of antimicrobial-resistant bacteria, particularly *Staphylococcus aureus*, which rapidly develops multidrug resistance and commonly colonizes wound surfaces, demands innovative strategies. Phage-encoded endolysins offer a dual-purpose approach as topical therapies for infectious skin wounds and synergistic agents to reduce high-dose antibiotic dependence. This study explores recombinant CHAPk (rCHAPk), efficiently synthesized within 3 h, displaying broad-spectrum antibacterial activity against 10 Gram-positive strains, including resistant variants, with rapid bactericidal kinetics. Application of 10 μg of rCHAPk reduced OD_{600} by 0.4 within 5 min against a clinical methicillin-resistant *S. aureus* (MRSA) strain. Combining rCHAPk (1.875 μg/mL) with oxacillin/vancomycin lowered their minimum bactericidal concentrations to 1 μg/mL from initial values over 64 μg/mL and 32 μg/mL, respectively, with a fractional inhibitory concentration index below 0.1. rCHAPk retained efficacy after one year of refrigerated storage. In *in vivo* experiments, rCHAPk outperformed commercial fucidin therapy in MRSA-induced murine wound models over two weeks, enhancing wound healing by modulating pro-inflammatory cytokine responses and the proliferative phase. This study, for the first time, investigates rCHAPk's *in vitro* combination with antibiotics and wound healing parameters, highlighting its potential as a potent antibacterial agent synergizing with antibiotics to address antibiotic-resistant bacterial wound infections.

1. Introduction

Bacteriophages, bacterial viruses, have been used for over 100 years to treat bacterial infections, including various ESKAPE members [1]. However, phage therapy faces several challenges in many countries, including issues with pharmaceutical production, dosing control, immunogenicity, the potential for horizontal gene transfer, resistance, and legal barriers [2]. Around 20 years ago, researchers initiated exploring the potent bactericidal activity of phage-encoded antibacterial enzymes, also referred to as endolysins or enzybiotics, which could overcome the limitations mentioned [3]. Endolysins, characterized by their primary role in peptidoglycan degradation, serve as crucial agents facilitating the liberation of nascent phages from bacterial cells, thereby contributing to the progression of the phage lytic cycle [4]. When endolysins are produced and purified by recombinant protein technology and then exogenously treated into Gram-positive bacteria, they cause external lysis, resulting in the death of the bacteria [2,5,6]. Endolysins, unlike antibiotics, exhibit superior functionality as an

Abbreviations: rCHAPk, recombinant CHAPk; MRSA, methicillin-resistant *S. aureus*; ΣFIC, fractional inhibitory concentration index; MIC, minimum inhibitory concentration); MBC, minimum bactericidal concentration; TR, turbidity reduction.

* Corresponding author.
E-mail address: tulin.ozbek@yildiz.edu.tr (T. Ozbek).

https://doi.org/10.1016/j.ijbiomac.2025.139630
Received 2 June 2024; Received in revised form 24 December 2024; Accepted 6 January 2025
Available online 7 January 2025

'active mode of action' [7], and are also characterized by high enzymatic activity, pathogen specificity, structural and activity diversity, low propensity for bacterial resistance development, stability over a broad pH and temperature spectrum, and efficacy in biofilms and mucosal surfaces, often synergizing with various antibacterial agents [8–13]. Phages are natural components of the human microbiota, therefore, the release of phage-derived endolysins is unlikely to have a detrimental effect on human health [14]. They can be administered into the body *via* different routes of drug delivery, such as topical (creams, ointments, and gels), parenteral (intravenous or intraperitoneal), oral, transnasal, or vaginal [2,15]. Endolysins have been tested in various animal models to combat bacterial infections in animals and humans. They have undergone clinical trials in recent years [7]. Clinical trials began eight years after the first successful *in vivo* trial in 2001, and as of 2021, some commercial enzymes are in the final phase of testing. Enzybiotic-based commercial products are predicted to become widespread in the near future, with increased use in clinical, food, and agriculture settings [3,7,16].

The focus of this study is the CHAP (cysteine- and histidine-dependent amidohydrolase/peptidase), domain of the LysK enzyme, which was identified in the genome of bacteriophage K (ATCC, 19685-B1), a polyvalent broad host range antistaphylococcal phage [17]. In 2009, it was demonstrated that the truncated enzyme (CHAPk) had about twice the activity of LysK [18]. The following year, rapid progress was made with the first *in vivo* study showing that CHAPk eliminated *S. aureus* in the nares of mice [19]. In an *ex vivo* experiment, CHAPk application on pig skin effectively eradicated 2.5×10^5 CFU/cm^2 bacteria [20]. Recent studies have focused on examining its antibiofilm activity across diverse strains, encompassing hospital-associated and bovine-derived MRSA [21,22]. As the skin and mucosal membranes are the two main reservoirs of *S. aureus* in humans and animals, and MRSA is one of the leading resistant organisms in healthcare settings, studies on the elimination of MRSA in the nasal passages and on the skin surface are currently popular [23–26].

The current investigation not only corroborates earlier research findings but also researches into, for the first time, the synergistic interaction of the rCHAPk enzyme with three distinct antibiotics *in vitro*, and its application in a murine model of MRSA-infected wounds comparison with commercial Fucidin.

2. Materials & methods

2.1. Microorganisms and the growth conditions

S. aureus (ATCC 25923) was utilized to propagate bacteriophage K (ATCC® 19,685-B1™) in Brain Heart Infusion (BHI) broth using the double-layer agar technique [27] and zymogram assay. Transformed *Escherichia coli* BL21 (DE3) was used for protein expression and grown on Lysogeny Broth (LB) agar plates or in LB broth supplemented with ampicillin (100 μg/mL). Microorganisms that were mentioned in Table 1 are from the culture collection of the Microbiology Laboratory at the Department of Molecular Biology and Genetics, Yıldız Technical University, were used for TR (turbidity reduction) assays. Additionally, a clinical MRSA strain was utilized for MIC (minimum inhibitory concentration)/ MBC (minimum bactericidal concentration), shelf-life, and *in vivo* experiments. For all bacteria, the optimum growth temperature condition was 37 °C. The L929 mouse fibroblast cell line used for biocompatibility assay is from Yeditepe University's Cell Culture Laboratory.

2.2. Cloning of CHAPk domain from the lysK gene

Gene *lysK* from phage K was previously identified (NCBI GeneID: 19622106) [28], elucidated its domains [17] (Fig. S1), and the 3-D structure of CHAPk (PDB no: 4CSH, [29]). The CHAPk sequence from *lysk* gene was amplified by PCR using Phusion High-Fidelity DNA Polymerase (Thermo scientific- F530L) (forward primer: 5′GGTGATGATGATGACAAGGCTAAGACTCAAG3′, reverse primer: 5′GGAGATGGGAAGTCATTATGCTTTTACAGG3′), and inserted into the pLATE51 vector of the aLICator LIC Cloning & Expression System cloning kit (Thermo scientific- K1251, Thermo Fisher Scientific, MA, USA) according to the kit instructions. The obtained ligation product was transformed into chemically prepared competent *E. coli* BL21 (DE3) cells, and the resulted colonies were selected through colony PCR, then the confirmed recombinant plasmids were extracted with QIAprep Spin Miniprep Kit (Qiagen-Cat. No. 27104), and analyzed through Sanger sequencing for further confirmation.

Table 1
Tested microorganisms and their sensibility results against rCHAPk.

Bacteria	Strain characteristics	rCHAPk effect	Indicated on TR graphs as:
S. aureus	ATCC 25923	Positive	*S. aureus* ATCC 25923
S. aureus	RN4220	Positive	*S. aureus* RN4220
S. aureus	ATCC 67101, Methicillin-resistant	Positive	MRSA
S. aureus	ATCC BAA-2419, Methicillin-susceptible Isolated from wound source	Positive	MSSA
S. aureus	ATCC 25923, Oxacillin-susceptible	Positive	MOSSA
S. aureus	ATCC 43300, Methicillin-oxacillin-resistant	Positive	MORSA
Staphylococcus epidermidis	Resistance phenotype: E, AMC, P, AM Isolated from milk source	Positive	*S. epidermidis* food strain 1
Staphylococcus epidermidis	Isolated from milk source	Positive	*S. epidermidis* food strain 2
Staphylococcus chromogenes	Isolated from milk source	Positive	*S. chromogenes*
Listeria monocytogenes	Isolated from food source	Negative	*Listeria monocytogenes*
S. aureus	Clinical strain, Methicillin-resistant, Resistance phenotype: FOX (diameter: 12 mm)	Positive	MRSA clinical strain
Bacillus cereus	ATCC 10876	Negative	
Bacillus subtilis	ATCC 6633	Negative	
Enterococcus faecalis	Resistance phenotype: P, AM Isolated from milk source	Negative	
E. faecalis	Resistance phenotype: SXT, P, AM Isolated from milk source	Negative	
E. faecalis	ATCC 51299, Vancomycin-resistant	Negative	
E. coli	ATCC 25922	Negative	

FOX = cefoxitin; E, erythromycin; AMC, amoxicillin-clavulanic acid; P, penicillin G; AM, ampicillin; SXT, trimethoprim-sulfomethoxazole.

2.3. Expression, purification, and concentration of rCHAPk protein

E. coli BL21 cells transformed with pLATE51 including CHAPk insert were grown at 37 °C in 50 mL of LB medium supplemented with 100 μg/mL of ampicillin until reaching an OD_{600} = 0.5–0.7. 1 mM of IPTG (isopropyl-β-D-thiogalactopyranoside) was used to induce rCHAPk (recombinant CHAPk) protein expression, and cells were harvested after induction for 3 h at 28 °C 220 rpm. Crude of intracellular protein lysate from induced culture resuspended in the PBS (20 mM sodium phosphate buffer and 300 mM NaCl pH:7.4) was produced by cell disruption using both lysozyme (1 mg/mL) treatment and sonication for 8 min on ice (60 % power and 10 s on/ 15 s off). His-tagged rCHAPk from the protein lysate was purified under native conditions using the Ni-NTA Purification System (Thermo Fisher Scientific) according to the manufacturer's instructions, where rCHAPk was recovered in elution buffer (PBS with

400 mM imidazole) [30]. The eluents were concentrated against 10 mM sodium acetate buffer (pH 7.0) using an Amicon® Ultra-15 Centrifugal Filter Unit (MWCO.10 K; Millipore) and following quantified using Bradford assay (Bio-Rad).

2.4. SDS-PAGE, zymogram, and Western blot assay

The concentrated protein was run on two of the 20 % SDS-PAGE gels (Bio-Rad, Hercules, USA), and one of them was visualized with then Coomassie Brilliant Blue R-250 staining (Bio-Rad). Another gel containing mid-log phase *S. aureus* (ATCC 25923), as a substrate, was used for zymogram analysis. In the assay, Donovan et al.'s method was conducted with minor modifications [31]. After electrophoresis, the gel was soaked in distilled water for 10 min, in 2.5 % Triton X-100 (*v*/v) for 20 min, and in distilled water two times for 30 min, then incubated in PBS overnight. Clearness against a turbid background is an indication of enzymatic activity. For the Western blot assay, the concentrated protein was run by 15 % SDS-PAGE and the proteins on the gel were transferred onto the nitrocellulose membrane (Thermo Fisher Scientific). His-probe Antibody (H-3): sc-8036 primary antibody (Santa Cruz Biotechnology, Dallas, USA) and Goat anti-Mouse IgG (H + L) secondary antibody (Invitrogen, MA, ABD) were used for marking and chromogenic visualization of the rCHAPk with His-tag [32].

2.5. In vitro antibacterial analyses of rCHAPk

2.5.1. Determining the host range of rCHAPk through TR assay and evaluating its activity at various initial substrate concentrations

The enzymatic activity of rCHAPk was determined using a Microplate Spectrophotometer (BioTek Epoch 2) through a TR assay. The tested bacteria (refer to Table 1) were grown at 37 °C and 180 rpm until they reached an optical density at 600 nm (OD_{600}) of 0.6–0.7. The cells were then pelleted by centrifugation and resuspended in 10 mM sodium acetate buffer (pH 7.0). For MRSA (clinical strain) only, the culture was also diluted to an OD_{600} of 0.25 and 0.12 with the same buffer and the maximum velocity of an enzymatically catalyzed reaction was calculated (see Fig. S4 for equations). A volume of 100 μL of rCHAPk at five different concentrations (10 μg, 6 μg, 3 μg, 1.5 μg, and 0.75 μg, corresponding to 2.28 μM, 1.37 μM, 0.68 μM, 0.34 μM, and 0.17 μM, respectively) was added to 100 μL of bacterial cultures prepared in the same buffer within the wells of a 96-well microplate. Absorbance values were obtained at 5-min intervals for 1 h at 37 °C at 600 nm. Gram-negative *Escherichia coli* (ATCC 25922) was evaluated as a negative control, and the blank control was carried out by adding 10 mM sodium acetate buffer (pH 7.0) without the enzyme in the assay. Experiments involving 17 different bacteria and 5 different enzyme concentrations were independently performed in triplicate. The reduction curves were created using spectrophotometric measures, and also bacterial reduction was confirmed with standard plate counts on Baird-Parker Agar (BPA, Laborlar Biyoteknoloji, Turkey) supplemented with egg yolk tellurite and Tyriptic Soy Agar (TSA, Merck, Germany) plates.

2.5.2. MIC/MBC assays of rCHAPk-antibiotic combinations

The antimicrobial activity of rCHAPk was assessed using a broth microdilution assay against clinical MRSA. The assay was conducted following the Clinical & Laboratory Standards Institute (CLSI) standard [33], with some modifications due to the non-activation of rCHAPk in Mueller-Hinton broth (MHB, Merck, Germany). Clinical MRSA was first grown in MHB at 37 °C for 4–6 h. They were then diluted to 5×10^5 CFU/mL in 10 mM sodium acetate buffer (pH 7.0) for use in this study. The rCHAPk was tested at concentrations ranging from 1.875 to 50 μg/mL prepared in 10 mM sodium acetate buffer (pH 7.0). After 2 h of treatment with the protein (only buffer was used for bacteria control), the bacteria were harvested by centrifugation. Finally, the pellets were resuspended in MHB and transferred into wells of a 96-well plate. The plate was then incubated at 37 °C and the absorbance values (OD_{600}) were recorded in real-time at 30-min intervals for 18 h. The growth curves of left MRSA after enzyme treatment were created using spectrophotometric measures, and also bacterial reduction was confirmed with standard plate counts on TSA plates. All experiments were independently conducted in triplicate.

To determine the synergetic effect of ampicillin/vancomycin/oxacillin antibiotics and rCHAPk on MRSA, MIC (minimum inhibitory concentration) and MBC (minimum bactericidal concentration) values of the antibiotics were first determined using the previously described broth microdilution method [34]. Fifteen different reactions for each antibiotic were carried out based on the three lowest concentrations (7.5–3.75-1.875 μg/mL; 0.342–0.171-0.086 μM, respectively) of rCHAPk and the MIC values of the antibiotics, as well as the four values below the determined MICs. The previously mentioned method was used exactly, but antibiotics were added after the pellet resuspension with the MHB step. The fractional inhibitory concentration (FIC) index (Σ) of the antibiotic and rCHAPk was calculated using the following equation [35]:

$$\Sigma\mathrm{FIC} = \mathrm{FIC}_{\mathrm{rCHAPk}} + \mathrm{FIC}_{\mathrm{antibiotic}} \quad (\mathrm{FIC}_{\mathrm{rCHAPk}} = \mathrm{MIC}_{\mathrm{rCHAPk\ with\ antibiotic}}/\mathrm{MIC}_{\mathrm{rCHAPk}}, \mathrm{FIC}_{\mathrm{antibiotic}} = \mathrm{MIC}_{\mathrm{antibiotic\ with\ rCHAPk}}/\mathrm{MIC}_{\mathrm{antibiotic}}) \tag{1}$$

A ΣFIC value of ≤0.5 indicates a synergistic interaction between the two substances.

2.6. Shelf-life analysis

Given the importance of the enzyme for commercial use, the activity of rCHAPk in 10 mM sodium acetate buffer (pH 7.0) stored in the refrigerator (4–8 °C) was tested at a concentration of 2.28 μM using the TR analysis described above on clinical MRSA strain for 1 year at different time intervals. At the end of the reaction setup, samples were spread onto BPA, and incubated overnight at 37 °C. The surviving bacteria were counted the following day by observing visible colonies. In this study, only buffer treatment was used as a control. Each experiment was independently performed in triplicate. The logarithmic reduction and killing percentage of the gels on the test organisms were calculated to measure antibacterial activity [36]:

$$\mathrm{Reduction}, \%(\mathrm{CFU/mL}) = \frac{\mathbf{B} - \mathbf{A}}{\mathbf{B}} \times \mathbf{100} \tag{2}$$

$$\mathrm{Log_{10}\ reduction} = \mathbf{Log_{10}}\ (\mathbf{B}) - \mathbf{Log_{10}}\ (\mathbf{A}) \tag{3}$$

where, **A:** CFU per milliliter for the well containing bacteria treated with rCHAPk, and **B:** CFU per milliliter for the "bacteria control" well untreated.

2.7. Determination of the endotoxin level and in vitro cytotoxicity assay

Endotoxin contamination of 500 μg/mL purified rCHAPk was measured using a PierceTM Chromogenic Endotoxin Quant Kit (ThermoFisher Scientific), according to the manufacturer's instructions. The biocompatibility of rCHAPk was evaluated using the MTT method on L929 (ATCC CCL-1) mouse fibroblast cells. The cells were cultured in

RPMI1640 medium supplemented with 10 % fetal bovine serum (FBS) and antibiotics (100 U/mL penicillin and 100 μg/mL streptomycin) under standard conditions (37 °C, 5 % CO_2) in flasks [37,38]. Cell viability was assessed using trypan blue before the cytotoxicity test, achieving a range of 93–95 %. The cells were then seeded in 96-well plates at a density of 5×10^4 cells/well and grown as sub-confluent monolayers at 37 °C in 5 % CO_2. The culture medium was subsequently replaced with varying concentrations of rCHAPk (2–200 μg/mL), and the plates were incubated for 24 h under the same conditions. All experiments were independently performed in triplicate, and cell viability was measured spectrophotometrically at OD_{590} nm and calculated using the following formula [39]:

$$\text{cell viability\%} = [(\mathbf{A1} - \mathbf{A2})/(\mathbf{B1} - \mathbf{B2})] \times 100 \quad (4)$$

where **A1** is the absorbance value from wells with rCHAPk, **A2** is the absorbance value of the blank well containing culture medium with the corresponding rCHAPk concentration, **B1** is the absorbance value of untreated control cells, and **B2** is the absorbance value of the blank well containing culture medium.

2.8. In vivo experiments of rCHAPk

2.8.1. Animals and housing

All animal procedures and experiments conducted in this study adhered strictly to national guidelines for the ethical use and care of laboratory animals. The Kastamonu University local animal care committee approved the study under reference number E-16498365-050.06.04-2300092798/(04.09.2023). A total of 132 male BALB/c mice aged 6–8 weeks and weighing between 25 and 30 g were procured from the Kastamonu University Experimental Research and Application Unit. The mice were housed in standard plastic cages lined with sawdust bedding within a climate-controlled environment set at 22 ± 1 °C, subjected to lighting conditions alternating between 12-hour periods of light and darkness, and fed *ad libitum* standard laboratory chow and water.

2.8.2. Experimental design and treatment

The main hypothesis aimed to determine whether differences could be identified among the experimental groups. Changes in cytokine levels were considered the primary outcome variable. Based on an effect size of 0.50, α = 0.05, and power = 0.8, with three measurement points in the wound model (days 3, 7, and 14), and 8 experimental groups, a total sample size of over 110 animals was calculated using G*Power 3.1.9.7. This corresponds to 5 animals per endpoint. To ensure that potential animal loss would not compromise the total sample size, the initial number of animals was increased by 20 %. The mice were randomly separated into 8 main groups: Healthy (Control, $n = 6$), Wound formation (W, $n = 18$), Wound formation + Fucidin treatment (W + Fucidin, n = 18), MRSA infected wound model (W ± MRSA, n = 18), Animal Model + Fucidin treatment (W ± MRSA+Fucidin, n = 18), Animal Model +50 μg rCHAPk treatment (CHAPk-50, n = 18), Animal Model +100 μg rCHAPk treatment (CHAPk-100, n = 18), Animal Model +200 μg rCHAPk treatment (CHAPk-200, n = 18). The mice were anesthetized intraperitoneally using a mixture of 1.6 mL xylazine (20 mg/kg) and 5 mL ketamine (100 mg/mL) at a dose of 0.01 mL per animal. They were then positioned in a prone orientation on a sterile surgical drape. The dorsal region was shaved and cleansed with 2 mL of 0.9 % saline solution without the use of any chemical agents or antiseptics. A full-thickness wound measuring 8 mm in diameter was created along the dorsal midline using sterile tissue scissors with curved blades. The surgical procedure was conducted at room temperature and adhered to aseptic principles. For the creation of the MRSA-induced wound model, MRSA (clinical isolate) stored in a stock solution was cultured afresh in a petri dish utilizing Mueller Hinton agar (Sigma-Aldrich). Following sufficient proliferation, colonies obtained from the medium *via* a swab were diluted in 0.9 % isotonic NaCl solution, and a dosage of 1×10^8 CFU/100 μL was inoculated into each wound area. The application of topical formulations commenced three days post-bacterial inoculation, upon establishment of infection within the wound area. Subsequent applications were conducted every 12 h over a period of 14 days. Fucidin (Fucidin 2 % cream) served as a positive control and was administered concurrently with other formulation applications in accordance with its prescribed instructions. At the termination of the experimental period at days 0, 3, 7, and 14, the animals underwent photographic documentation. On days 3, 7, and 14, six mice from each group were administered euthanasia with a high dose, subsequently, excision areas measuring 4 × 2 cm were meticulously removed. The tissue from each animal was reserved for molecular, biochemical, and histopathological investigations.

2.9. Biochemical analysis

Tissue samples obtained from each mouse were pulverized in liquid nitrogen using a TissueLyser II grinding jar set (Qiagen, Hilden, Germany). Approximately 100 mg of pulverized tissue was homogenized with TissueLyser II (Qiagen) in 1 mL of PBS homogenate buffer within an Eppendorf tube, followed by centrifugation. Measurements were conducted using the Commercial Kit method following the manufacturer's protocol. Superoxide dismutase (SOD) activity (Cat No. Eo290Mo, BT LAB ELISA KIT, Shanghai Korain Biotech, China), glutathione (GSH) levels (Cat No. E0394Mo, BT LAB ELISA KIT, Shanghai Korain Biotech, China), and malondialdehyde (MDA) levels (Cat No. E0625Mo, BT LAB ELISA KIT, Shanghai Korain Biotech, China) were quantified in each sample supernatant and standards using previously established enzyme-linked immunosorbent assay (ELISA) methods at room temperature [40]. A standard curve was generated, and an equation was derived from the absorbance of the standards. Linear SOD, GSH, and MDA concentrations were calculated based on this equation and expressed as U/mg protein, nmol/mg protein, and nmol/mg protein, respectively. The obtained data were presented as mean ± standard deviation (SD) per 1 mg of protein. All measurements were performed in triplicate. All chemicals utilized were of analytical grade and were procured from Sigma-Aldrich (Germany).

2.10. Molecular analysis

2.10.1. Total RNA extraction and cDNA synthesis

The scar tissue was preserved in RNA Stabilization Solution and stored at −80 °C before being pulverized in liquid nitrogen using a TissueLyser II (Qiagen, Hilden, Germany). Approximately 35 μg of pulverized tissue was homogenized with TissueLyser II (Qiagen) in 350 μL of RLT-buffered homogenate buffer within an Eppendorf tube, followed by centrifugation. Total RNA isolation was carried out using the RNeasy Mini Kit (Qiagen) according to the manufacturer's instructions, utilizing Qiaqube (Qiagen). The purified total RNA was subsequently reverse transcribed into complementary DNA (cDNA) employing the High Capacity cDNA Reverse Transcription Kit (Applied Biosystems, Foster City, CA, USA), following procedures outlined in our previous study [41].

2.10.2. Relative quantification of the gene expression

Relative expression analyses of COL1A, FGF2, MMP9, NF-κβ, TGFβ1, TNFα, and VEGFA were conducted using Real-Time Reverse Transcriptase PCR and the StepOnePlus Real-Time PCR System (Applied Biosystems). The PCR reactions utilized Primer Perfect Probe mix and TaqMan Probe-based technology (Primer Design Ltd., Southampton, UK). For each cell group, triplicate determinations were performed for both targets in a 96-well optical plate. Each 20 μL reaction mixture contained 9 μL of cDNA (100 ng), 1 μL of Primer Perfect Probemix, and 10 μL of QuantiTect Probe PCR Mastermix (Qiagen, Hilden, Germany). The thermal cycling conditions were as follows: an initial heating step at

50 °C for 2 min, followed by 95 °C for 10 min, and 40 cycles consisting of 15 s at 94 °C and 60 s at 60 °C. Results were presented as the relative fold change in expression compared to control animals. Gene transcripts, including COL1A, FGF2, MMP9, NF-κβ, TGFβ1, TNFα, and VEGFA, were amplified using mouse-specific primers (Table S1). The housekeeping gene β-actin was used for the normalization of gene expression levels (Mm02619580_g1). The PCR procedure followed the manufacturer's protocol and was consistent with the previous study [42]. Gene expression data were analyzed using the $2^{-\Delta\Delta Ct}$ method and presented as fold-change relative to the animal groups [43]. All analysis was performed in triplicate.

2.11. Histological analysis

Following the dissection of the rats, skin tissues were procured and subsequently fixed in 10 % buffered neutral formaldehyde for 72 h. These tissues underwent dehydration *via* a graded alcohol series, were embedded in paraffin wax, and sectioned to a thickness of 5 μm utilizing a Leica RM2125RT microtome (Leica Microsystems, Wetzlar, Germany). Subsequently, for histopathological analysis, the sections were subjected to staining with hematoxylin-eosin, followed by examination under a light microscope equipped with a camera (Olympus BX43 with DP21 camera system). The evaluation of the wound healing process was conducted across two distinct phases. The Inflammation Phase encompassed the assessment of exudate fields to gauge capillary permeability, examination of inflammation areas to ascertain leukocyte migration, and observation of granulation tissue formation indicative of granulomatous response. In contrast, the Proliferation Phase involved the evaluation of angiogenesis, activation of fibroblasts denoting collagen synthesis, and the formation of a new matrix. These assessments were systematically carried out and are summarized in Table 2.

2.12. Statistical analysis

The statistical software used for data analysis was IBM SPSS version 27.0.1 (IBM, Armonk, NY, USA). Descriptive statistics were presented as 'number (n)', 'percentage (%)', 'mean', and 'standard deviation (SD)'. One-way ANOVA–Duncan's and Tukey's tests were used to analyze all numerical, independent data with more than two groups. Graphs were created using GraphPad Prism version 10.1.0 (GraphPad Software, San Diego, California, USA). All the *p*-values were based on a two-sided test of statistical significance. Differences between groups were considered significant ($p < 0.05$).

3. Results & discussion

3.1. Achieved rapid large-scale production of rCHAPk in a short period

The truncated endolysin CHAPk has a known endopeptidase activity on the pentaglycine cross-bridge of the peptidoglycan layer of *S. aureus* [44], therefore this activity can be utilized for exogenous treatment on *S. aureus* or other cells that have similar cell surface organization by decreasing cell wall stiffness and integrity due to a reduced level of peptidoglycan cross-linking. Based on this function, the *in vitro* antibacterial activity of the rCHAPk enzyme produced in our study was measured against various bacteria at different concentrations. Additionally, its synergy with antibiotics was examined using the MRSA clinical strain, which is highly sensitive to rCHAPk. It is widely

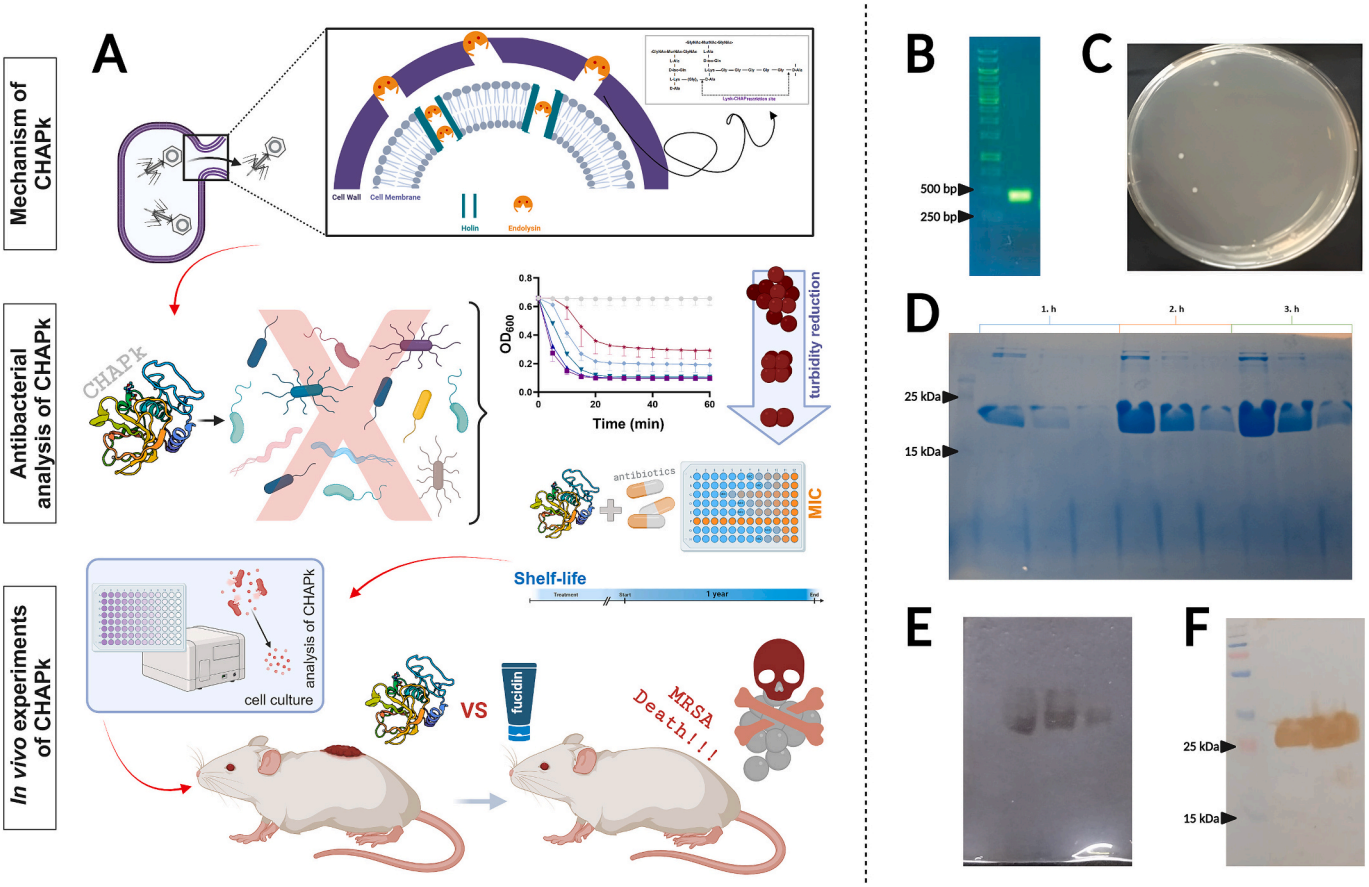

Fig. 1. A Schematic representation of the study workflow (created with BioRender.com), B the CHAPk sequence amplicon, C the clone cells transformed with the CHAPk-inserted plasmid, D SDS-PAGE result of rCHAPk expressed at 1 h, 2 h, and 3 h first three elution fractions from purification step, respectively, E and F zymogram assay and Western blot result of rGp45, respectively.

acknowledged that the commercial value of a pharmaceutical product is determined by its shelf-life, toxicity, and bioactivity. Considering this, all culture and *in vivo* studies were conducted in a controlled manner (Fig. 1A).

During the initial step of the research, CHAPk sequence was amplified as 495 bp in length which is the first 495 nucleotide of *lysK* gene (Fig. 1B), *E. coli* BL21 (DE3) transformed with the CHAPk-inserted pLATE51 was obtained (Fig. 1C) and the clones were validated both colony PCR (Fig. S2) and sequence analysis which was revealed no base differences or frameshifts of the CHAPk sequence on the plasmid (Fig. S3), and finally, N-terminus 6 × His-tagged rCHAPk was successfully overexpressed for 3 h and purified using the nickel-NTA column at the predicted molecular mass of 21.95 kDa (Fig. 1D). At 28 °C, significant increases in protein expression were observed during the first 1 to 3 h of induction, with no appreciable differences in yield detected between 3, 4, and 6 h (Fig. S6). The combination of a 1 mM IPTG concentration and an induction period within the 3- to 6-h range demonstrated compatibility with the 28 °C incubation condition, yielding consistent and reproducible protein expression. In zymogram analysis which was performed by *co*-polymerizing *S. aureus* ATCC 25923 into the gel matrix, a clear band on the turbid background due to the cell substrate indicating enzymatic activity was observed in the same size region (Fig. 1E). The protein was also confirmed by Western blot assay utilizing the polyhistidine tail (Fig. 1F) and at an amount of approximately 7 mg using the Bradford assay in a single expression process.

3.2. rCHAPk is effective against 10 different microorganisms including those that are resistant, its activity increases with the amount of substrate used, and there is a high synergistic effect between low-concentration rCHAPk and antibiotics

TR assays (Fig. 2) clearly demonstrate that rCHAPk had an antibacterial effect on 11 different strains of the tested microorganisms (Table 1), including 3 resistant, 3 different species of the same genus, and 1 different genus. The antibacterial effect increased as the concentration increased from 0.375 μg to 10 μg in all experiments studied, with no significance difference between 6 μg (1.37 μM) and 10 μg (2.28 μM) ($p > 0.05$), especially for MOSSA, MORSA, *S. epidermidis* food strain 1, and MRSA clinical strain ($p > 0.9$). As the application time increased, the amount of substrate digested decreased after an average of 20 min. However, two bacteria stand out at this point; MOSSA and MRSA clinical strain (all concentrations have p -values below 0.001). An average decrease of 0.3 and 0.4 OD_{600} was achieved in the first 5 min for 10 and 6 μg treatment, respectively. Therefore, after the first 10 min, the amount of substrate in the environment is much less compared to the other studied groups. Since analysis of all results indicated the highest enzyme activity on the MRSA clinical strain, this strain was chosen as the reference for further analysis. When comparing host range and dose studies with other investigations involving rCHAPk, the literature consistently demonstrates its efficacy across a broad spectrum of hosts [21,45]. This broad effectiveness is a characteristic trait of Gram-positive endolysins, which is due to the structure of the Gram-positive cell surface [46,47]). Furthermore, the rCHAPk enzyme's solitary catalytic domain inherently displays increased and less specific activity when lacking a CBD [18]. This phenomenon cannot be avoided. Notably, studies such as the one conducted by Fenton et al. [45] demonstrate that CHAPk exhibits activity even at very low doses. For example, their study on *S. aureus* DPC5246 showed a 70 % kill rate with only 10 μg of protein in just 5 min [45]. This is similar to the 65–70 % effectiveness observed on MRSA clinical strains in our current study. Additionally, similar studies have demonstrated CHAPk's effectiveness against a wide range of species and genera [21,45]. Consistent with these findings, our study confirms the broad-spectrum activity by demonstrating efficacy against different strains.

When analyzing enzyme activity based on the initial substrate amount (Fig. 2B), it was observed that the velocity decreased as the

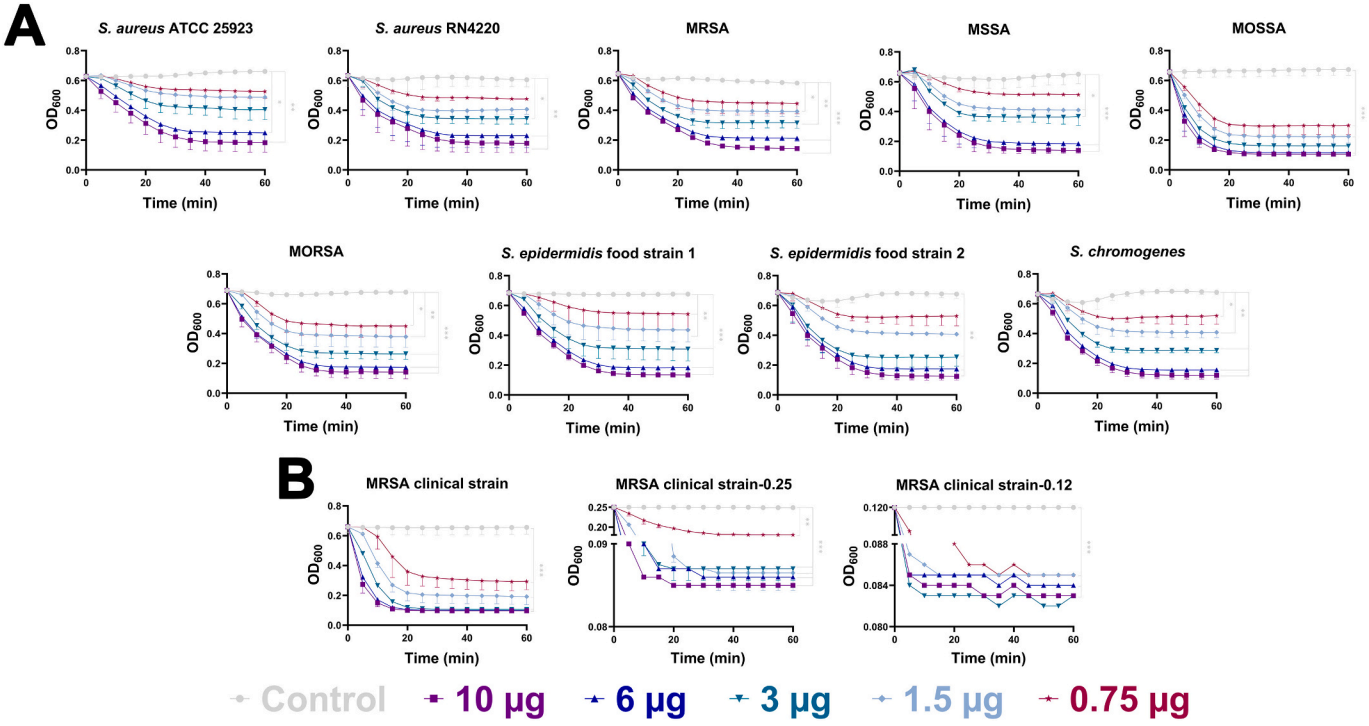

Fig. 2. The TR assay yielded results from two experiments: A, which involved testing various strains with an average initial substrate concentration, and B, which focused on the reference clinical strain MRSA with varying initial substrate concentrations (for enhanced readability of the graph, the baseline was set at 0.08, reflecting the absorbance value of approximately 0.083 obtained from the blank control). The p-values are shown as $p < 0.05$(*), $p < 0.01$(**), and $p < 0.001$(***) to denote the statistical significance of the OD decrease compared to the control. The error bars indicate the standard deviation from the mean, with a sample size of $n = 3$.

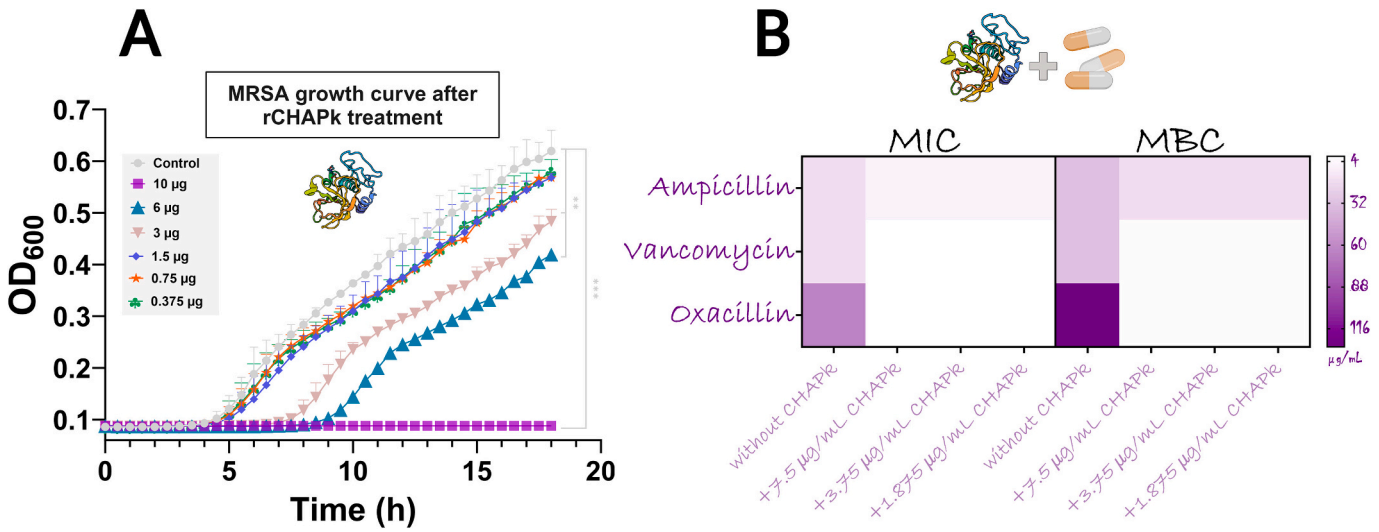

Fig. 3. Graphs presenting antimicrobial data from only rCHAPk treatment and in combination with antibiotics. A The growth curves of MRSA cells treated with rCHAPk per 200 µL reaction, with absorbance values recorded every half hour over 18 h, are presented. The *p*-values are presented as $p < 0.01$(**) and $p < 0.001$(***) to indicate the statistical significance of the OD reduction relative to the control. The error bars represent the standard deviation from the mean, derived from a sample size of $n = 3$. B Depicting MIC/MBC values of only antibiotic and rCHAPk/antibiotic synergism on clinical MRSA strain. The colour scale, ranging from white to dark purple, reflects increasing antibiotic concentrations from 1 µg/mL to 128 µg/mL. The first column of both the MIC and MBC fields shows the values of the reaction in the absence of rCHAPk for the antibiotics alone, while the subsequent columns represent the decreasing concentrations of rCHAPk added.

number of binding cells decreased to the enzyme, calculated as 0.17 for 0.6 OD_{600}, 0.1 for 0.25 OD_{600}, and 0.09 for 0.12 OD_{600} in the reaction setting up with 10 µg rCHAPK (Fig. S4). However, almost all the substrate in the reaction was digested within one hour for the initial amount of 0.12 OD_{600}. The same result was observed for all initial amounts except for the lowest amount of enzyme at the initial amount of 0.25 OD_{600}. For the initial amount of 0.65 OD_{600}, there were still undigested bacteria at the end of the reaction.

Applying only rCHAPk resulted in a bactericidal effect on bacteria at 50 µg/mL (MBC). At 30 µg/mL (MIC) and 15 µg/mL, a bacteriostatic effect was observed, and a delay in bacterial lag-phase of 4 h 19 min, and 3 h occurred, respectively (Fig. 3A). The antibacterial effect at 7.5–3.75-1.875 µg/mL was found to be minimal (1 h delay in lag-time and an average OD_{600} decrease of 0.035) when compared to the growth of the control without rCHAPk treatment (Fig. 3A). Although this effect may seem unimportant, it raises the question of whether high antibiotic synergism can be achieved with the lowest concentrations of the enzyme, and also considering the economic value of low doses for a commercial drug. Therefore, the study investigated the antibacterial effects of antibiotics when combined with the three lowest concentrations of rCHAPk. First, the MIC/MBC values of the MRSA clinical strain for each antibiotic were determined as follows: 16 µg/mL MIC - 32 µg/mL MBC for ampicillin, 16 µg/mL MIC - 32 µg/mL MBC for vancomycin, and 64 µg/mL MIC - >64 µg/mL MBC for oxacillin. Fig. 3B shows that all combinations of rCHAPk concentrations resulted in a considerable reduction of the MIC/MBC values for the synergetic effect. The new MBC values for oxacillin and vancomycin were 1 µg/mL, whereas the new MIC value for ampicillin was 8 µg/mL and the MBC was 16 µg/mL (Fig. S5). The ΣFIC value is 0.56 for rCHAPk and ampicillin, but it is below 0.1 for rCHAPk and oxacillin/vancomycin, indicating a considerably high synergetic effect [48]. Upon reviewing the literature, several studies concerning *S. aureus* and MRSA support our findings. Kim et al. [35] reported synergy between SAL200 and vancomycin across various *S. aureus* strains [35]. Likewise, Kashani et al. [49] confirmed highly synergistic interactions between CHAP-amidase and vancomycin for MRSA252, with a ΣFIC value of 0.375 [49]. Daniel et al. observed ΣFIC values of <0.5 for both interactions involving ClyS endolysin, vancomycin, and oxacillin on vancomycin-intermediate strains of *S. aureus* (VISA) and MRSA [50]. These investigations collectively underscore the notable synergistic effects of vancomycin and oxacillin in conjunction with endolysins on resistant *S. aureus* strains. Our study has successfully demonstrated synergy between rCHAPk and three distinct antibiotics against a clinical MRSA strain for the first time in the literature. We recommend further investigations focusing on the combined application of rCHAPk with vancomycin and oxacillin.

Endolysins have an active mode of action that differs from antibiotics, as they clear not only dividing cells but also all bacteria present in the environment. When the enzyme combines with the substrate, rapid digestion occurs. Saturation can be observed in the TR graphs in Fig. 2 if the enzyme is not re-added to the medium. As a solution to this situation, combined approaches with commercially available antibiotics can reduce the development of resistance and provide economic benefits. Based on our study, clinical studies can be conducted with two types of scenarios: (i) based on the growth inhibition shown in Fig. 3A, it is recommended to administer daily repeated doses of endolysin treatment alone. The advantage of endolysins is that their catalytic domains directly target vital components of the bacterial wall [51]. Although the remodeling of the bacterial wall structure raises concerns about an evolutionary change episode of the bacterium, there is a possibility of a loss in the sustainability of its life activity [51]. The bacterium is unlikely to develop resistance, as supported by studies in the literature [52,53]. Therefore, considering that the activity of the enzyme may decrease due to the *in vivo* environment, *in vitro* active doses of the enzyme can be given at regular intervals (1–12 h intervals according to the graph for our study). In this method we chose for the *in vivo* model, rCHAPk was applied on a wound model, and considering the pH, temperature, *etc.* conditions around the wound [54], the doses of 50 µg/mL, 100 µg/mL, and 200 µg/mL will be given twice a day at 12 h intervals, taking the inhibition dose of the enzyme in broth microdilution as reference [51] µg/mL); (ii) an alternative proposal involves the concurrent examination of endolysins and antibiotics. To mitigate the necessity for elevated antibiotic dosages amidst the resistance crisis, a synergistic dual antibacterial approach can be effectively deployed [55,56], a premise substantiated by our *in vitro* investigation. For conditions such as acne or other dermatological infections, implementing a co-prescription regimen wherein rCHAPk is administered initially, followed by antibiotics after a 2-h interval, presents a viable therapeutic strategy. This approach is in line with the crucial role of current

antibiotics as essential agents in fighting bacterial infections, despite the fact that we are currently in a post-antibiotic era. In the context of managing financial ramifications stemming from epidemics/pandemics triggered by resistant bacterial strains and curtailing the resurgence of resistance, advocating for distinct targeted or mechanistic pharmaceutical models offers a promising avenue for biocontrol. This advocacy is supported by utilizing current resources and the capabilities of recombinant DNA technology, enabling cost-effective large-scale production [57].

3.3. rCHAPk maintained its enzymatic activity for a year, and its low endotoxin level and biocompatibility make it suitable for in vivo and clinical research

For therapeutic proteins to be considered a valid product, the desired shelf-life stability is usually between 2 and 3 years at 2–8 °C which is the intended commercial storage temperature [58,59]. Fig. 4B-C shows that rCHAPk remained active with an average 5.23 log-reduction/99.8 % kill rate after being refrigerated (4–8 °C) for one year, emphasizing its therapeutic efficiency (it is been kept in the same condition for further examination). In comparison to Fenton et al.'s study, which observed a rapid loss of activity after 2 months of CHAPk stored in sterile water at 4 °C [45], the rCHAPk that we produced has demonstrated significant stability for 1 year. It is possible that storing the enzyme in a buffer solution may be a more effective strategy [60]. The endotoxin level of the rCHAPk product was determined to be 0.75 EU/mL. This value is well below the accepted threshold of 20 EU/mL for biomedical applications, indicating the product's suitability for use in therapeutic and diagnostic contexts [61]. The MTT cell viability assay results demonstrate the effect of rCHAPk on L929 cell viability. The bioavailability of rCHAPk was determined by comparing the percentage of viable cells to untreated control cells. A bioavailability threshold of 70 % was used to interpret the results, as per established literature [62,63]. Therefore, the results indicate that rCHAPk treatments did not induce any toxic effects on L929 cells at all tested doses, and there were no substantial changes in cell viability after 24 h. The low level of endotoxin, and cell culture viability of over 70 % underscore the quality and safety of the rCHAPk protein, emphasizing its potential for use in various therapeutic applications.

3.4. Comparing therapeutics and control groups showed that rCHAPk significantly promoted faster healing by reducing pro-inflammatory cytokine response and accelerating the wound healing proliferative phase

For macroscopical evaluation, Fig. 5A summarizes the example photographs from each group that demonstrate wound closure ratios in a day-dependent manner. Compared to all the treated groups, a significantly higher wound healing was observed in the group treated with 200 μg rCHAPk until the 14th day. Also, lower doses were effective and all three doses' wound healing effects were better than fucidin's. Upon examination of the skin tissue sections for microscopic evaluation, it was observed that the epidermis had ulceration, leukocyte infiltration in the dermal area, chronic inflammation, and necrotic foci. In contrast, the Control group sections exhibited a normal appearance as expected, without any wounds. Significant effects were noted on the epidermis in both the W and the W + MRSA groups, characterized by ulceration and severe dermal inflammation on days 3 and 7. However, on the 14th day of the experiment, a partial reduction in this damage was observed,

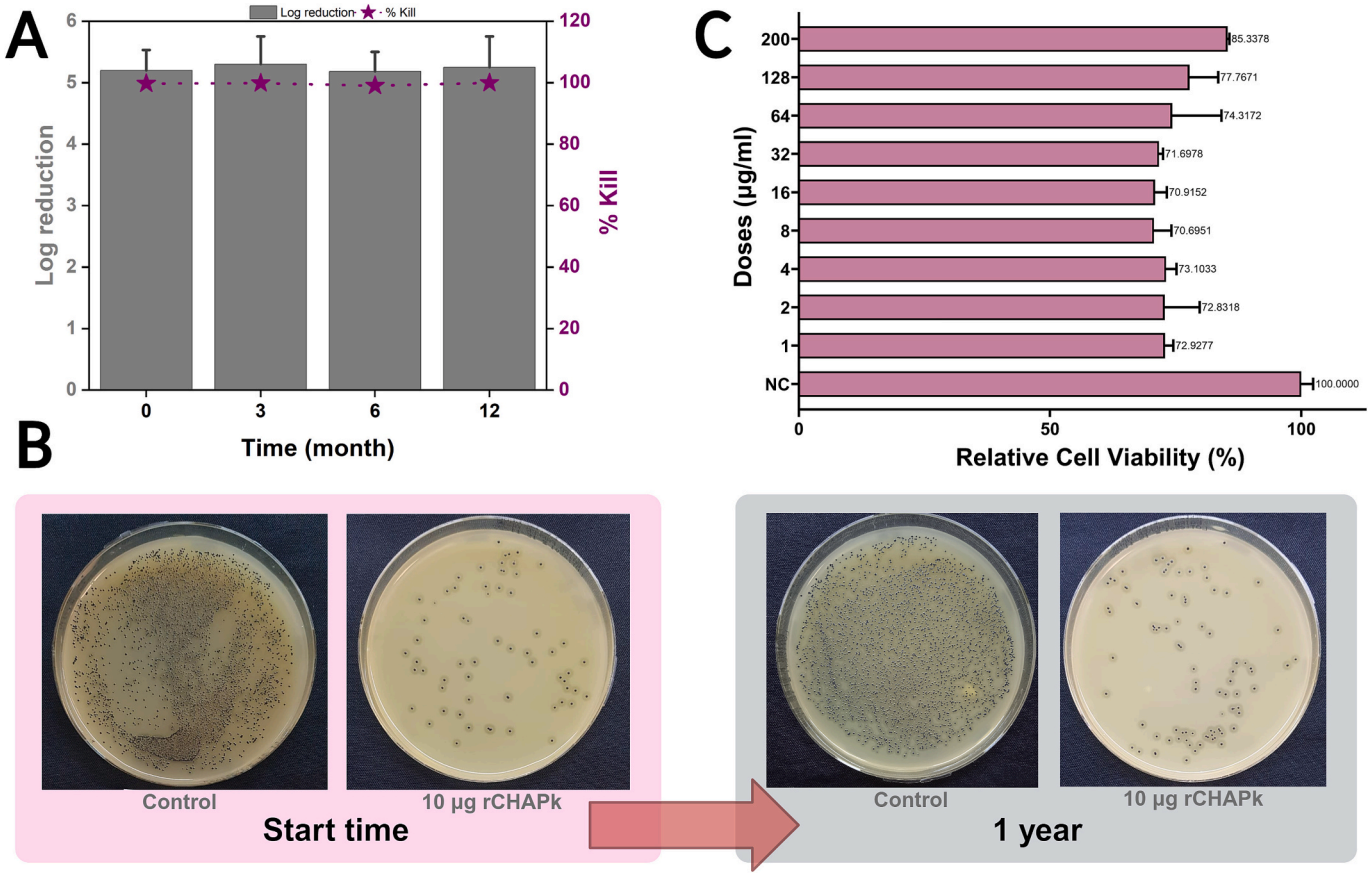

Fig. 4. Shelf-life and biocompatibility analysis of rCHAPk. A The graph of the log-reduction and percentage of bacteria killed by rCHAPk over a period of one year at three-month intervals, measured by B the colony count of the remaining bacteria in the reaction with/without rCHAPk, respectively (due to similar results, only the colony images from the first and last-12th month were shared). C The biocompatibility assessment outcome of rCHAPk for 24 h.
The error bars denote the standard deviation from the mean, based on a sample size of $n = 3$.

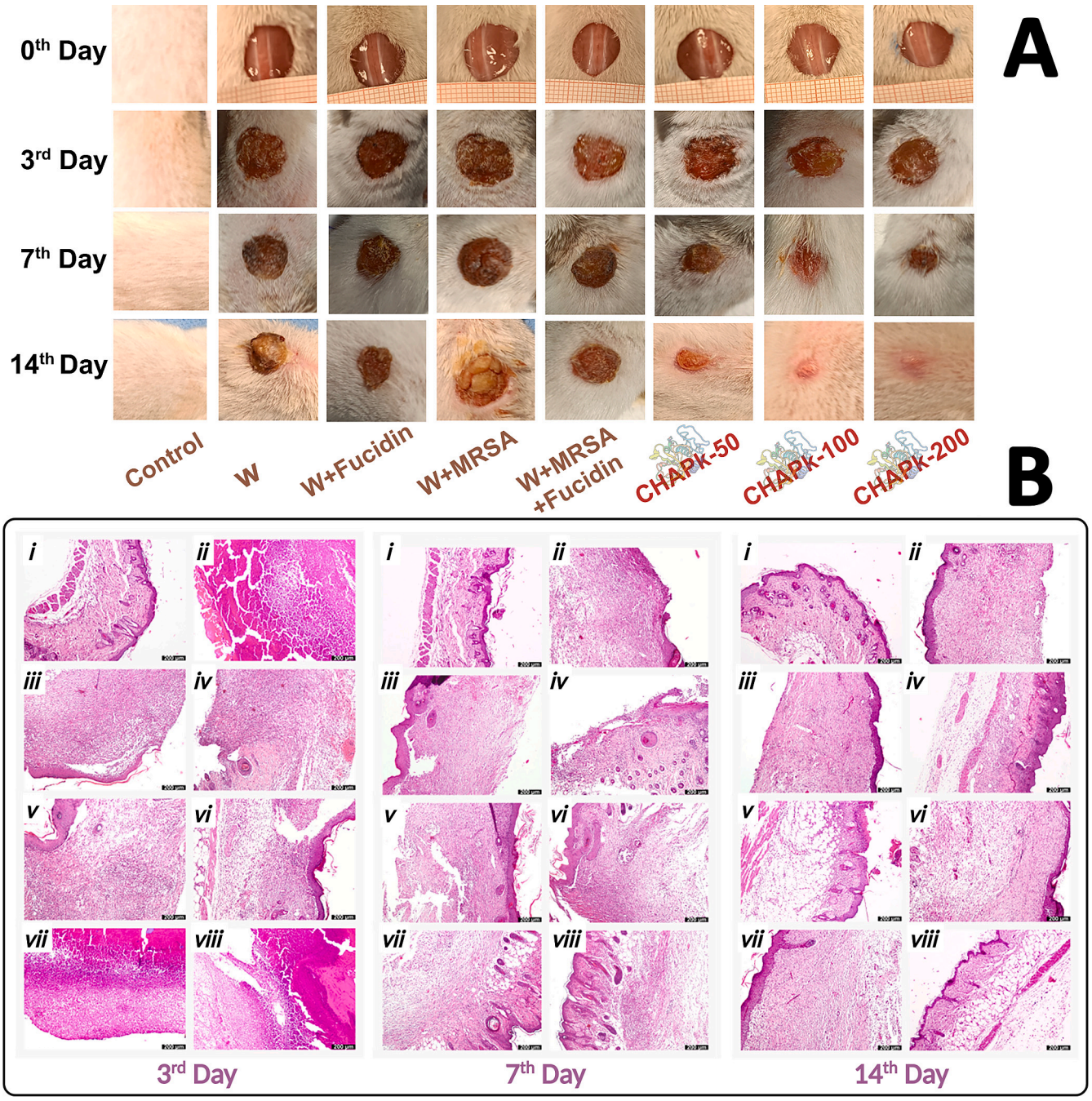

Fig. 5. Macroscopic and microscopic evaluations of wound areas before and after euthanasia of mice. A Macrophotographs depicting wound progression in each experimental group at 0, 3, 7, and 14 days post-wounding. B Appearance of histopathological changes of skin tissues from wound regions observed on the 3rd, 7th and 14th days, respectively. *i*. Control, *ii*. W, *iii*. W + Fucidin, *iv*. W + MRSA, *v*. W + MRSA+Fucidin, *vi*. CHAPk-50, *vii*. CHAPk-100, and *viii*. CHAPk-200 groups. Dye: Hematoxylin-Eosin, Bars = 200 μm.

indicating a spontaneous healing process in the rats. The inflammation in the dermis decreased, epithelialization commenced, and matrix reformation occurred progressively from the 3rd to the 14th day in the W + Fucidin, W + MRSA+Fucidin, and CHAPk (50-100-200 μg) groups. Significantly, the most notable improvement was observed on the 14th day with rCHAPk administered at 200 μg. All histopathological changes are seen in Fig. 5B. The semi-quantitative scoring for the inflammatory and proliferative phases across all experimental groups was compiled in Table 2. According to the table, the total inflammation scores, encompassing capillary permeability, leukocyte infiltration, and granulomatous scores, were notably elevated in the W and W + MRSA groups, while exhibiting lower values in the Fucidin and CHAPk groups, particularly at a dosage of 200 μg of rCHAPk on the 14th day. Conversely, the total proliferation scores, including angiogenesis, collagen synthesis, and matrix formation, were diminished in the W and W + MRSA groups, while displaying a progressive increase in a day-dependent manner in the CHAPk-200. Furthermore, the results indicated Fucidin's efficacy in both the W and W + MRSA groups; nevertheless, the CHAPk-200 exhibited superior total inflammation and proliferation scores on the 14th day compared to the Fucidin groups.

In summary, both macroscopical and microscopical evaluations suggest that the CHAPk-200 group displayed the most efficacious healing, likely due to the sustained presence of rCHAPk within the infected wound area throughout the 14-day period. Our investigation

Table 2
Semi-quantitative assessment of histopathological changes in all experimental groups.

	Histopathological findings/Groups	Control group			Wound (W) group			W+Fucidine group			W+MRSA group		
Inflammation Phase	**Exudate fields** *(Capillary permeability)*	0	0	0	4	1	1	2	1	0	3	3	0
	Inflammation areas *(Leukocyte migration)*	0	0	0	4	2	2	3	1	1	4	2	2
	Granulation tissue formation *(Granulomatous)*	0	0	0	2	2	1	2	1	1	4	2	1
	ΣInflammation Score	**0**	**0**	**0**	**10**	**5**	**4**	**7**	**3**	**2**	**11**	**7**	**3**
Proliferation Phase	**Angiogenesis**	0	0	0	0	2	2	1	2	4	0	2	3
	Activation of fibroblasts *(Collagen synthesis)*	0	0	0	0	3	3	0	3	3	0	2	3
	New matrix formation	0	0	0	0	1	3	0	3	3	0	1	2
	ΣProliferation Score	**0**	**0**	**0**	**0**	**6**	**8**	**1**	**8**	**10**	**0**	**5**	**8**
		3. day	**7. day**	**14. day**	**3. day**	**7. day**	**14. day**	**3. day**	**7. day**	**14. day**	**3. day**	**7. day**	**14. day**
	Histopathological findings/Groups	**W+MRSA+Fucidine group**			**CHAPk-50 group**			**CHAPk-100 group**			**CHAPk-200 group**		
Inflammation Phase	**Exudate fields** *(Capillary permeability)*	3	1	0	3	2	0	4	1	0	2	0	0
	Inflammation areas *(Leukocyte migration)*	3	1	1	3	2	1	3	1	1	3	1	0
	Granulation tissue formation *(Granulomatous)*	2	2	0	3	1	1	2	1	0	2	1	0
	ΣInflammation Score	**8**	**4**	**1**	**9**	**5**	**2**	**9**	**3**	**1**	**7**	**2**	**0**
Proliferation Phase	**Angiogenesis**	0	2	4	0	2	2	0	2	3	0	3	3
	Activation of fibroblasts *(Collagen synthesis)*	0	3	3	0	2	3	0	3	3	0	3	4
	New matrix formation	0	1	3	0	1	3	0	3	3	0	4	4
	ΣProliferation Score	**0**	**6**	**10**	**0**	**5**	**8**	**0**	**8**	**9**	**0**	**10**	**11**
		3. day	**7. day**	**14. day**	**3. day**	**7. day**	**14. day**	**3. day**	**7. day**	**14. day**	**3. day**	**7. day**	**14. day**

0 = none, 1 = slight, 2 = moderate, 3 = severe, 4 = more severe.

identified the reduction of inflammation, re-epithelialization, and matrix formation as pivotal indicators of the healing process. Consistent efficacy outcomes of endolysins in MRSA-induced wound models support our findings, potentially stemming from the action of endolysins in phage-mediated bacterial lysis. Additionally, the extant literature on wound models treated with endolysins targeting *S. aureus* and MRSA substantiates our observations. Noteworthy, the effectiveness of CPPTat-JDlys fusion endolysin was demonstrated by the observation of moderate epidermal necrosis and cellulitis in lysin-treated mice after 5 days, followed by accelerated epidermal regeneration and progressive wound healing by day 8 in MRSA-induced murine skin infections [64]. Moreover, XZ.700, formulated as a cream, demonstrates significant efficacy in eradicating *S. aureus* on reconstituted human epidermis, while the application of a chimeric enzyme XZ.700-containing gel leads to a notable reduction in bacterial colonization in a murine model of *S. aureus*-induced skin infection compared to untreated controls [65]. Combination therapy with endolysin MR-10 and minocycline surpasses endolysin monotherapy, which is also effective, in treating burn wound infections, resulting in rapid wound closure and reduced inflammation, approximately 98 % wound contraction by the 12th day, followed by complete closure within around 14 days [66]. These findings support the utilization of endolysin-based treatments, such as rCHAPk, to fasten wound healing and combat MRSA infections.

Fig. 6 presents data on the activity of superoxide dismutase (SOD), levels of reduced glutathione (GSH), and concentrations of malondialdehyde (MDA) in skin tissues. The wound model was established *via* MRSA application, and the presence of the antioxidant enzyme SOD, GSH, and oxidative product MDA was observed in all experimental groups. A decline in skin SOD activities and GSH levels over time ($p < 0.05$) was observed in the healthy group compared to others, particularly evident in the W + MRSA group. Conversely, MDA levels showed a significant increase in the W + MRSA group ($p < 0.05$) compared to the healthy control. Additionally, a notable increase in SOD activities and GSH levels was observed in all treatment groups when compared to the W + MRSA group. The CHAPk-200 group showed a significant approximation to the healthy control at day 14 ($p < 0.05$). Furthermore, the application of CHAPk-200 significantly reduced the increased MDA levels ($p < 0.05$) observed in the W + MRSA group, as shown in Fig. 6.

In this study, we investigated the mRNA expressions of COL1A, FGF2, MMP9, NF-κβ, TGFβ1, TNFα, and VEGFA utilizing RT-qPCR methodology. The mRNA expressions of these genes across the 3rd, 7th, and 14th day groups are shown in Fig. 6. Notably, in response to the application of W + MRSA, a discernible time-dependent escalation in the mRNA expressions of MMP9, NF-κβ, TGFβ1, and TNFα was observed ($p < 0.05$). Particularly noteworthy is the significantly heightened expression of these genes in the 14th day W + MRSA groups in comparison to both the 3rd and 7th day counterparts ($p < 0.05$). In conjunction with the W + MRSA application, a statistically significant time-dependent reduction was observed in the expressions of COL1A, FGF2, and VEGFA ($p < 0.05$). Notably, the expressions of these genes were significantly decreased in the 14th day W + MRSA group compared to both the 3rd and 7th day groups ($p < 0.05$). The administration of rCHAPk treatment significantly reduced the mRNA expression levels of MMP9, NF-κβ, TGFβ1, and TNFα compared to the W + MRSA groups at all time points assessed ($p < 0.05$). Additionally, rCHAPk treatment upregulated the mRNA expression levels of COL1A, FGF2, and VEGFA, which were downregulated by MRSA throughout the evaluated time points ($p < 0.05$). It is important to note that although other treatment groups (W + MRSA+Fucidin, CHAPk-50, and CHAPk-100) also showed improvement in the damage caused by the MRSA-induced wound model, the degree of improvement was not as significant as that observed in the CHAPk-200 group.

CHAPk has previously demonstrated antibacterial effects on pig skin [20]; however, its effect on wound healing parameters, such as oxidative stress, inflammatory cytokines and pathways, and growth factors directly contributing to all processes, has been investigated for the first time in this study. In one study, the GspA protein, which contains the CHAP domain and catalyzes the hydrolysis of Gsp to GSH and spermidine, was found to play an important role in redox sensing and protein S-thiolation [67]. The enzymatic process in which rCHAPk contributes may be responsible for supporting oxidative balance in the wound area. By evaluating SOD activity and MDA levels, we can observe the balance achieved. MDA, as an end-product of lipid peroxidation and degradation, accumulates in the wound area, and rCHAPk scavenges this end-product by increasing SOD enzyme and glutathione levels, which are well-known antioxidant agents [68]. In this study, we also examined inflammatory markers, as the wound healing process involves different steps: (i) coagulation and hemostasis; (ii) inflammation; (iii)

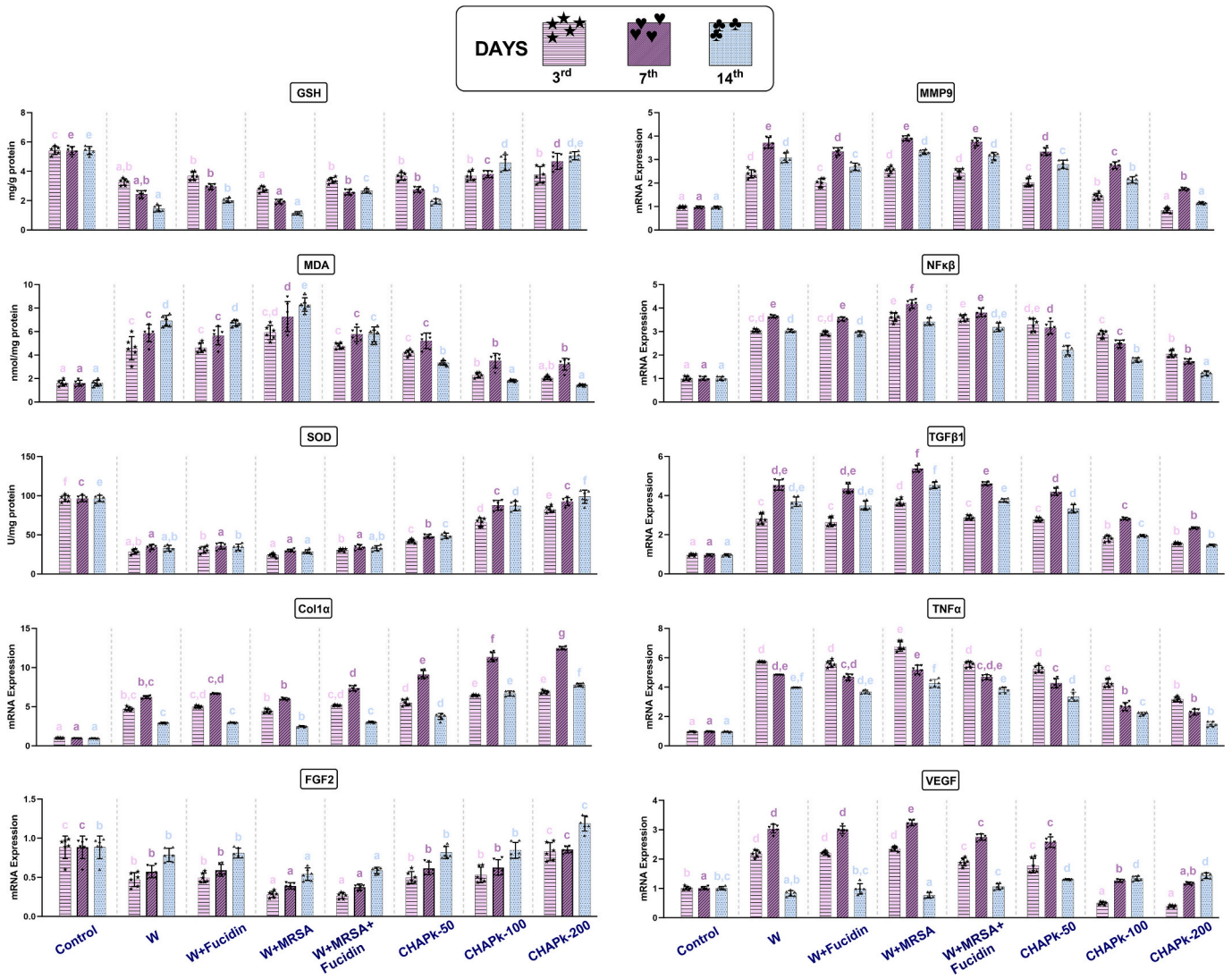

Fig. 6. Oxidative stress parameters (SOD, GSH, MDA) and relative mRNA expression levels of pro-inflammatory cytokines (COL1A, FGF2, MMP9, NF-κβ, TGFβ1, TNFα, and VEGFA) in wound tissues. Statistical analysis using Duncan's multiple range test identified significant differences between groups on the same day, denoted by different letters (a, b, c, d, e, f) above the columns. Values with distinct letters differ significantly ($p < 0.05$), while those sharing the same letters do not ($p > 0.05$). The third day is represented by light magenta columns with horizontal stripes, the seventh day by dark magenta columns with sloping lines, and the fourteenth day by light blue columns with dots. The letters indicating statistical significance correspond to the column colors for each day. Relative expression levels were calculated using the $2^{-\Delta\Delta Ct}$ method. Each value represents the mean ± S.D. for six samples per group.

proliferation; and (iv) wound remodeling with scar tissue formation [69]. To evaluate all steps of the wound healing process, we assessed both inflammatory and proliferator parameters such as TNFα, NF-κB, MMP9, COL1A, FGF2, TGFβ1, and VEGFA. Previously, Bäuerl et al. [70] demonstrated that the genomes of *Lactobacillus casei/paracasei* and *Lactobacillus rhamnosus* strains carry genes encoding homologues of p40 and p75 from L. *rhamnosus* GG. These genes encode secreted proteins with CHAP and NLPC/P60 domains, which display anti-apoptotic and cell protective effects on human intestinal epithelial cells [70]. This finding supports our observation that rCHAPk prevents skin tissue damage. Additionally, in another study, Chopra et al. investigated the potential effects of combining MR-10, an endolysin product such as rCHAPk, with well-known antibacterial agents to treat MRSA-induced systemic and localized burn wound infections in mice. They suggested that MR-10 supported wound healing by decreasing oxidative stress and supporting collagen formation [66]. In contrast to the findings of Chopra et al., our study demonstrated a distinct enhancement in wound healing solely through the application of rCHAPk, devoid of adjunctive administration with a well-known antibacterial agent. Based on the results from the literature and our study, we can suggest that rCHAPk enhances wound healing not only by demonstrating antibacterial effects but also by supporting the steps of wound healing through anti-inflammatory and proliferative effects.

4. Conclusion

Phage-encoded endolysins have emerged as a promising approach to combat the looming antibiotic resistance crisis, which poses a significant threat to public health. These endolysins offer dual functionality as both a topical treatment for infectious skin wounds and a potent mediator of high synergism when combined with antibiotics. This dual functionality presents a potential solution to the challenge of developing novel antimicrobial strategies. The results of our *in vitro* study indicate that synergistic dual antibacterial approaches have the potential to alleviate the reliance on elevated antibiotic dosages, which is becoming increasingly challenging due to the escalating antimicrobial resistance crisis. Notably, rCHAPk exhibits remarkable efficacy against MRSA-induced wounds, which warrants further clinical evaluation and the

exploration of its dual applications alongside established antibiotics in rigorous *in vivo* investigations.

CRediT authorship contribution statement

Semra Tasdurmazli: Writing – original draft, Visualization, Methodology, Investigation, Formal analysis. **Irfan Cinar:** Writing – original draft, Methodology. **Murat Karamese:** Writing – original draft, Methodology. **Selina Aksak Karamese:** Writing – original draft, Methodology. **Elif Cadirci:** Writing – original draft, Data curation. **Luís D.R. Melo:** Writing – review & editing, Data curation. **Tulin Ozbek:** Writing – original draft, Validation, Supervision, Project administration.

Declaration of competing interest

The authors declare no conflict of interest.

Acknowledgements

We would like to thank Yeditepe University Medical Genetics Department and Dr. Utku Özbey for biocompatibility analyses. This article/publication is based upon work from COST Action EURESTOP, CA21145, supported by COST (European Cooperation in Science and Technology). Author Semra Tasdurmazli has been also granted a 2211-A scholarship (reference number 1649B032200498) by TUBITAK.

Appendix A. Supplementary data

Supplementary data to this article can be found online at https://doi.org/10.1016/j.ijbiomac.2025.139630.

References

[1] A. Patil, R. Banerji, P. Kanojiya, S. Koratkar, S. Saroj, Bacteriophages for ESKAPE: role in pathogenicity and measures of control, Expert Rev. Anti-Infect. Ther. 19 (2021) 845–865, https://doi.org/10.1080/14787210.2021.1858800.
[2] K.M. Danis-Wlodarczyk, D.J. Wozniak, S.T. Abedon, M. Sillankorva, Treating bacterial infections with bacteriophage-based enzybiotics: in vitro, in vivo and clinical application, Antibiotics 10 (2021) 1497, https://doi.org/10.3390/ANTIBIOTICS10121497.
[3] D. Nelson, L. Loomis, V.A. Fischetti, Prevention and elimination of upper respiratory colonization of mice by group A streptococci by using a bacteriophage lytic enzyme, Proc. Natl. Acad. Sci. USA 98 (2001) 4107, https://doi.org/10.1073/PNAS.061038398.
[4] C. São-José, Engineering of phage-derived lytic enzymes: improving their potential as antimicrobials, Antibiotics 7 (2018) 29, https://doi.org/10.3390/ANTIBIOTICS7020029.
[5] M. Schmelcher, D.M. Donovan, M.J. Loessner, Bacteriophage endolysins as novel antimicrobials, Future Microbiol. 7 (2012) 1147, https://doi.org/10.2217/FMB.12.97.
[6] L.D.R. Melo, A. Brandão, E. Akturk, S.B. Santos, J. Azeredo, Characterization of a new *Staphylococcus aureus* Kayvirus harboring a lysin active against biofilms, Viruses 10 (2018) 182, https://doi.org/10.3390/V10040182.
[7] E. Murray, L.A. Draper, R.P. Ross, C. Hill, The advantages and challenges of using endolysins in a clinical setting, Viruses 13 (2021) 680, https://doi.org/10.3390/V13040680.
[8] Y. Briers, R. Lavigne, Breaking barriers: expansion of the use of endolysins as novel antibacterials against Gram-negative bacteria, in: Doi:10.2217/Fmb.15.8 10, 2015, pp. 377–390, https://doi.org/10.2217/FMB.15.8.
[9] D. Dams, Y. Briers, Enzybiotics: enzyme-based antibacterials as therapeutics, Adv. Exp. Med. Biol. 1148 (2019) 233–253, https://doi.org/10.1007/978-981-13-7709-9_11.
[10] V.A. Fischetti, Development of phage lysins as novel therapeutics: a historical perspective, Viruses 10 (2018) 310, https://doi.org/10.3390/V10060310.
[11] Ł. Grabowski, K. Łepek, M. Stasiłojć, K. Kosznik-Kwaśnicka, K. Zdrojewska, M. Maciąg-Dorszyńska, G. Węgrzyn, A. Węgrzyn, Bacteriophage-encoded enzymes destroying bacterial cell membranes and walls, and their potential use as antimicrobial agents, Microbiol. Res. 248 (2021) 126746, https://doi.org/10.1016/J.MICRES.2021.126746.
[12] M. Guo, C. Feng, J. Ren, X. Zhuang, Y. Zhang, Y. Zhu, K. Dong, P. He, X. Guo, J. Qin, A novel antimicrobial endolysin, LysPA26, against Pseudomonas aeruginosa, Front. Microbiol. 8 (2017) 293, https://doi.org/10.3389/FMICB.2017.00293/BIBTEX.
[13] H. Yang, H. Zhang, J. Wang, J. Yu, H. Wei, A novel chimeric lysin with robust antibacterial activity against planktonic and biofilm methicillin-resistant *Staphylococcus aureus*, Sci. Rep. 7:1 7 (2017) (2017) 1–13, https://doi.org/10.1038/srep40182.
[14] A. Forde, C. Hill, Phages of life – the path to pharma, Br. J. Pharmacol. 175 (2018) 412–418, https://doi.org/10.1111/BPH.14106.
[15] M.T.P. Gontijo, G.P. Jorge, M. Brocchi, Current status of endolysin-based treatments against gram-negative bacteria, Antibiotics 10 (2021) 1143, https://doi.org/10.3390/ANTIBIOTICS10101143.
[16] S.Y. Jun, G.M. Jung, S.J. Yoon, M.D. Oh, Y.J. Choi, W.J. Lee, J.C. Kong, J.G. Seol, S. H. Kang, Antibacterial properties of a pre-formulated recombinant phage endolysin, SAL-1, Int. J. Antimicrob. Agents 41 (2013) 156–161, https://doi.org/10.1016/J.IJANTIMICAG.2012.10.011.
[17] S. O'Flaherty, A. Coffey, W. Meaney, G.F. Fitzgerald, R.P. Ross, The recombinant phage Lysin LysK has a broad Spectrum of lytic activity against clinically relevant staphylococci, including methicillin-resistant *Staphylococcus aureus*, J. Bacteriol. 187 (2005) 7161, https://doi.org/10.1128/JB.187.20.7161-7164.2005.
[18] M. Horgan, G. O'Flynn, J. Garry, J. Cooney, A. Coffey, G.F. Fitzgerald, R.P. Ross, O. McAuliffe, Phage lysin LysK can be truncated to its CHAP domain and retain lytic activity against live antibiotic-resistant staphylococci, Appl. Environ. Microbiol. 75 (2009) 872–874, https://doi.org/10.1128/AEM.01831-08.
[19] M. Fenton, P.G. Casey, C. Hill, C.G.M. Gahan, R.P. Ross, O. Mcauliffe, J. O'Mahony, F. Maher, A. Coffey, The truncated phage lysin CHAPk eliminates Staphylococcus aureus in the nares of mice, Bioeng. Bugs 1 (2010) 404, https://doi.org/10.4161/BBUG.1.6.13422.
[20] M. Fenton, R. Keary, O. McAuliffe, R.P. Ross, J. O'Mahony, A. Coffey, Bacteriophage-derived peptidase CHAPK eliminates and prevents staphylococcal biofilms, Int. J. Microbiol. 2013 (2013), https://doi.org/10.1155/2013/625341.
[21] Y. Shan, N. Yang, D. Teng, X. Wang, R. Mao, Y. Hao, X. Ma, H. Fan, J. Wang, Recombinant of the staphylococcal bacteriophage lysin CHAPk and its elimination against *Streptococcus agalactiae* biofilms, Microorganisms 8 (2020) 216, https://doi.org/10.3390/MICROORGANISMS8020216.
[22] M. Behera, G. Singh, A. Vats, M. Parmanand, D. Roshan, C. Gautam, R.K. Rana, S. Kesharwani, S.M. Ghorai De, Expression and characterization of novel chimeric endolysin CHAPk-SH3bk against biofilm-forming methicillin-resistant Staphylococcus aureus, Int. J. Biol. Macromol. 254 (2024) 127969, https://doi.org/10.1016/J.IJBIOMAC.2023.127969.
[23] E.M.H. Pallesen, M. Gluud, C.K. Vadivel, T.B. Buus, B. de Rooij, Z. Zeng, S. Ahmad, A. Willerslev-Olsen, C. Röhrig, M.R. Kamstrup, L. Bay, L. Lindahl, T. Krejsgaard, C. Geisler, C.M. Bonefeld, L. Iversen, A. Woetmann, S.B. Koralov, T. Bjarnsholt, J. Frieling, M. Schmelcher, N. Ødum, Endolysin inhibits skin colonization by patient-derived staphylococcus aureus and malignant T-cell activation in cutaneous T-cell lymphoma, J. Invest. Dermatol. 143 (2023) 1757–1768.e3, https://doi.org/10.1016/J.JID.2023.01.039.
[24] H.N. Wilkinson, A.R. Stafford, M. Rudden, N.D.C. Rocha, A.S. Kidd, S. Iveson, A. L. Bell, J. Hart, A. Duarte, J. Frieling, F. Janssen, C. Röhrig, B. de Rooij, P.F. Ekhart, M.J. Hardman, Selective depletion of Staphylococcus aureus restores the skin microbiome and accelerates tissue repair after injury, J. Invest. Dermatol. (2024), https://doi.org/10.1016/J.JID.2024.01.018.
[25] J.Y. Bae, K. Il Jun, C.K. Kang, K.H. Song, P.G. Choe, J.H. Bang, E.S. Kim, S.W. Park, H. Bin Kim, N.J. Kim, W.B. Park, M. don Oh, Efficacy of Intranasal Administration of the Recombinant Endolysin SAL200 in a Lethal Murine *Staphylococcus aureus* Pneumonia Model, Antimicrob Agents Chemother vol. 63, 2019, https://doi.org/10.1128/AAC.02009-18/ASSET/8BB74743-E12C-4452-B93C-24FD3419F5A6/ASSETS/GRAPHIC/AAC.02009-18-F0004.JPEG.
[26] G. Rahimzadeh, P. Gill, M. Saeedi, M. Ghasemi, G.R. Rokni, S.S. Rostamkalaei, A. A. Nadi Ghara, M.S. Rezai, Evaluation of bacteriophage products against burn wound Methicillin-resistant Staphylococcus aureus (MRSA) infections, Wound Med. 28 (2020) 100182, https://doi.org/10.1016/J.WNDM.2020.100182.
[27] B. Heshmati, I. Var, Isolation and Identification of Salmonella Bacteriophage from Sewage waters PhD Thesis View Project Investigation on Using of Apatogenic Aspergillus flavus for Reducing Aflatoxin Contamination in Corn Fields and Storage Conditions View Project. https://www.researchgate.net/publication/329736761, 2018.
[28] J.J. Gill, Revised genome sequence of Staphylococcus aureus bacteriophage K, Genome Announc. 2 (2014) 1173–1186, https://doi.org/10.1128/GENOMEA.01173-13.
[29] M. Sanz-Gaitero, R. Keary, C. Garcia-Doval, A. Coffey, M.J. Van Raaij, Crystal structure of the lytic CHAPKdomain of the endolysin LysK from Staphylococcus aureus bacteriophage K, Virol. J. 11 (2014) 1–11, https://doi.org/10.1186/1743-422X-11-133/FIGURES/5.
[30] S. Tasdurmazli, S. Dokuz, B. Erdogdu, I. Var, J.Y.S. Chen, T. Ozbek, The evaluation of biotechnological potential of Gp144, the key molecule of natural predator bacteriophage K in Staphylococcus aureus hunting mechanism, Biotechnol. J. (2023) 2300145, https://doi.org/10.1002/BIOT.202300145.
[31] S.M. Swift, D.T. Rowley, C. Young, A. Franks, P. Hyman, D.M. Donovan, The endolysin from the Enterococcus faecalis bacteriophage VD13 and conditions stimulating its lytic activity, FEMS Microbiol. Lett. 363 (2016) 216, https://doi.org/10.1093/FEMSLE/FNW216.
[32] T. Atabey, T. Acar, S. Derman, E. Ordu, A. Erdemir, P.N. Taşlı, G.K. Gür, F. Şahin, M. Güllüce, T. Arasoğlu, In vitro evaluation of immunogenicity of recombinant OMP25 protein obtained from endemic Brucella abortus Biovar 3 as vaccine candidate molecule against animal brucellosis, Protein Pept. Lett. 28 (2021), https://doi.org/10.2174/0929866528666210615104334.
[33] J.S. Lewis II, F.J. Amy Mathers, D.M. April Bobenchik, D. Alexandra Lynn Bryson, D. Shelley Campeau, D.K. Sharon Cullen, R. Tanis Dingle, F.F. Marcelo Galas, R. M. Humphries, F.J. Thomas Kirn, B. Limbago, V.M. Pierce, F.S. Sandra Richter, F. Michael Satlin, M.N. Audrey Schuetz, D. Susan Sharp, F.J. Patricia Simner, D.D.

Pranita Tamma, M.P. Melvin Weinstein, CLSI M100-Ed34 February 2024 Replaces CLSI M100-Ed33 Performance Standards for Antimicrobial Susceptibility Testing. https://clsi.org/terms-of-use/, 2024 (accessed March 8, 2024).
[34] T. Arasoglu, S. Derman, B. Mansuroglu, Comparative evaluation of antibacterial activity of caffeic acid phenethyl ester and PLGA nanoparticle formulation by different methods, Nanotechnology 27 (2015) 25103, https://doi.org/10.1088/0957-4484/27/2/025103.
[35] N.H. Kim, W.B. Park, J.E. Cho, Y.J. Choi, S.J. Choi, S.Y. Jun, C.K. Kang, K.H. Song, P.G. Choe, J.H. Bang, E.S. Kim, S.W. Park, N.J. Kim, M.D. Oh, H. Bin Kim, Effects of phage endolysin SAL200 combined with antibiotics on staphylococcus aureus infection, Antimicrob. Agents Chemother. 62 (2018), https://doi.org/10.1128/AAC.00731-18/SUPPL_FILE/ZAC010187501S1.PDF.
[36] ASTM International, E2149 Standard Test Method for Determining the Antimicrobial Activity of Antimicrobial Agents Under Dynamic Contact Conditions. https://www.astm.org/e2149-20.html, 2020. (Accessed 17 March 2024).
[37] H. Shapourian, M. Ghanadian, N. Eskandari, A. Shokouhi, G.Y. Demirel, A. V. Bazhin, M. Ganjalikhani-Hakemi, TIM-3/Galectin-9 interaction and glutamine metabolism in AML cell lines, HL-60 and THP-1, BMC Cancer 24 (2024) 1–15, https://doi.org/10.1186/S12885-024-11898-3/FIGURES/9.
[38] A. Taheri, S.E. Mobaser, P. Golpour, M. Nourbakhsh, M. Tavakoli-Yaraki, S. Yarahmadi, M. Nourbakhsh, Hesperetin attenuates the expression of markers of adipose tissue fibrosis in pre-adipocytes, BMC Complement. Med. Ther. 23 (2023) 1–11, https://doi.org/10.1186/S12906-023-04152-Z/FIGURES/6.
[39] J. van Meerloo, G.J.L. Kaspers, J. Cloos, Cell Sensitivity Assays: The MTT Assay, 2011, pp. 237–245, https://doi.org/10.1007/978-1-61779-080-5_20.
[40] R.A. Ugan, E. Cadirci, Z. Halici, E. Toktay, I. Cinar, The role of urotensin-II and its receptors in sepsis-induced lung injury under diabetic conditions, Eur. J. Pharmacol. 818 (2018) 457–469, https://doi.org/10.1016/J.EJPHAR.2017.11.011.
[41] I. Cinar, M. Yayla, T. Tavaci, E. Toktay, R.A. Ugan, P. Bayram, H. Halici, In vivo and in vitro cardioprotective effect of gossypin against isoproterenol-induced myocardial infarction injury, Cardiovasc. Toxicol. 22 (2022) 52–62, https://doi.org/10.1007/S12012-021-09698-3/FIGURES/6.
[42] I. Cinar, B. Sirin, P. Aydin, E. Toktay, E. Cadirci, I. Halici, Z. Halici, Ameliorative effect of gossypin against acute lung injury in experimental sepsis model of rats, Life Sci. 221 (2019) 327–334, https://doi.org/10.1016/J.LFS.2019.02.039.
[43] K.J. Livak, T.D. Schmittgen, Analysis of relative gene expression data using real-time quantitative PCR and the 2−ΔΔCT method, Methods 25 (2001) 402–408, https://doi.org/10.1006/METH.2001.1262.
[44] S. Arroyo-Moreno, M. Begley, K. Dembicka, A. Coffey, Engineering of the chapk staphylococcal phage endolysin to enhance antibacterial activity against stationary-phase cells, Antibiotics 10 (2021) 722, https://doi.org/10.3390/ANTIBIOTICS10060722/S1.
[45] M. Fenton, R.P. Ross, O. Mcauliffe, J. O'Mahony, A. Coffey, Characterization of the staphylococcal bacteriophage lysin CHAPK, J. Appl. Microbiol. 111 (2011) 1025–1035, https://doi.org/10.1111/J.1365-2672.2011.05119.X.
[46] F. Abdelrahman, M. Easwaran, O.I. Daramola, S. Ragab, S. Lynch, T.J. Oduselu, F. M. Khan, A. Ayobami, F. Adnan, E. Torrents, S. Sanmukh, A. El-Shibiny, Phage-Encoded Endolysins, Antibiotics 10 (2021) 124, https://doi.org/10.3390/ANTIBIOTICS10020124.
[47] D.C. Nelson, M. Schmelcher, L. Rodriguez-Rubio, J. Klumpp, D.G. Pritchard, S. Dong, D.M. Donovan, Endolysins as antimicrobials, Adv. Virus Res. 83 (2012) 299–365, https://doi.org/10.1016/B978-0-12-394438-2.00007-4.
[48] Amy L. Leber, Synergism testing: broth microdilution checkerboard and broth macrodilution methods, Clin. Microbiol. Proc. Handb. 5.16.1-5.16.23 (2016), https://doi.org/10.1128/9781555818814.CH5.16.
[49] H.H. Kashani, H. Fahimi, Y.D. Goli, R. Moniri, A novel chimeric endolysin with antibacterial activity against methicillin-resistant Staphylococcus aureus, Front. Cell. Infect. Microbiol. 7 (2017) 251764, https://doi.org/10.3389/FCIMB.2017.00290/BIBTEX.
[50] A. Daniel, C. Euler, M. Collin, P. Chahales, K.J. Gorelick, V.A. Fischetti, Synergism between a novel chimeric lysin and oxacillin protects against infection by methicillin-resistant Staphylococcus aureus, Antimicrob. Agents Chemother. 54 (2010) 1603–1612, https://doi.org/10.1128/AAC.01625-09/SUPPL_FILE/SUPPLIMENTAL_DATA_COMBINED.PDF.
[51] R. Vázquez, E. García, P. García, Phage lysins for fighting bacterial respiratory infections: a new generation of antimicrobials, Front. Immunol. 9 (2018) 408341, https://doi.org/10.3389/FIMMU.2018.02252/BIBTEX.
[52] D.B. Gilmer, J.E. Schmitz, C.W. Euler, V.A. Fischetti, Novel bacteriophage lysin with broad lytic activity protects against mixed infection by streptococcus pyogenes and methicillin-resistant staphylococcus aureus, Antimicrob. Agents Chemother. 57 (2013) 2743–2750, https://doi.org/10.1128/AAC.02526-12/SUPPL_FILE/ZAC999101878SO1.PDF.
[53] V.A. Fischetti, Bacteriophage lytic enzymes: novel anti-infectives, Trends Microbiol. 13 (2005) 491–496, https://doi.org/10.1016/J.TIM.2005.08.007.
[54] Z. Wang, F. Qi, H. Luo, G. Xu, D. Wang, Inflammatory microenvironment of skin wounds, Front. Immunol. 13 (2022) 789274, https://doi.org/10.3389/FIMMU.2022.789274/BIBTEX.
[55] X. Li, Y. He, Z. Wang, J. Wei, T. Hu, J. Si, G. Tao, L. Zhang, L. Xie, A.E. Abdalla, G. Wang, Y. Li, T. Teng, A combination therapy of phages and antibiotics: two is better than one, Int. J. Biol. Sci. 17 (2021) 3573, https://doi.org/10.7150/IJBS.60551.
[56] P. Letrado, B. Corsini, R. DÍez-Martínez, N. Bustamante, J.E. Yuste, P. García, Bactericidal synergism between antibiotics and phage endolysin Cpl-711 to kill multidrug-resistant pneumococcus, Future Microbiol. 13 (2018) 1215–1223, https://doi.org/10.2217/FMB-2018-0077/ASSET/IMAGES/LARGE/FIGURE3.JPEG.
[57] N.K. Tripathi, Production and purification of recombinant proteins from Escherichia coli, ChemBioEng Rev. 3 (2016) 116–133, https://doi.org/10.1002/CBEN.201600002.
[58] D. Kuzman, M. Bunc, M. Ravnik, F. Reiter, L. Žagar, M. Bončina, Long-term stability predictions of therapeutic monoclonal antibodies in solution using Arrhenius-based kinetics, Sci. Rep. 11 (2021) 20534, https://doi.org/10.1038/S41598-021-99875-9.
[59] J. Schuster, A. Koulov, H.C. Mahler, P. Detampel, J. Huwyler, S. Singh, R. Mathaes, In vivo stability of therapeutic proteins, Pharm. Res. 2020 37:2 37 (2020) 1–17, https://doi.org/10.1007/S11095-019-2689-1.
[60] H.S. Liu, Y.C. Cheng, Stability enhancement of α-amylase by supercritical carbon dioxide pretreatment, Prog. Biotechnol. 16 (2000) 149–154, https://doi.org/10.1016/S0921-0423(00)80028-3.
[61] L.A. Brito, M. Singh, Acceptable levels of endotoxin in vaccine formulations during preclinical research, J. Pharm. Sci. 100 (2011) 34–37, https://doi.org/10.1002/JPS.22267.
[62] P. Tua-Ngam, T. Srikhirin, P. Roongrujimek, L929 Cell Cytotoxicity Associated with Experimental and Commercial Dental Flosses, 2017, https://doi.org/10.1088/1757-899X/265/1/012010.
[63] V. Cannella, R. Altomare, G. Chiaramonte, S. Di Bella, F. Mira, L. Russotto, P. Pisano, A. Guercio, Cytotoxicity evaluation of endodontic pins on L929 cell line, Biomed. Res. Int. 2019 (2019), https://doi.org/10.1155/2019/3469525.
[64] Z.F. Wang, L.C. Kong, Y. Liu, Q. Fu, Z.L. Cui, J. Wang, J.J. Ma, H.A. Wang, Y. X. Yan, J.H. Sun, A phage Lysin fused to a cell-penetrating peptide kills intracellular methicillin-resistant Staphylococcus aureus in keratinocytes and has potential as a treatment for skin infections in mice, Appl. Environ. Microbiol. 84 (2018), https://doi.org/10.1128/AEM.00380-18.
[65] F. Eichenseher, B.L. Herpers, P. Badoux, J.M. Leyva-Castillo, R.S. Geha, M. van der Zwart, J. McKellar, F. Janssen, B. de Rooij, L. Selvakumar, C. Röhrig, J. Frieling, M. Offerhaus, M.J. Loessner, M. Schmelcher, Linker-improved chimeric endolysin selectively kills Staphylococcus aureus in vitro, on reconstituted human epidermis, and in a murine model of skin infection, Antimicrob. Agents Chemother. 66 (2022), https://doi.org/10.1128/AAC.02273-21/SUPPL_FILE/AAC.02273-21-S0001.PDF.
[66] S. Chopra, K. Harjai, S. Chhibber, Potential of combination therapy of endolysin MR-10 and minocycline in treating MRSA induced systemic and localized burn wound infections in mice, Int. J. Med. Microbiol. 306 (2016) 707–716, https://doi.org/10.1016/J.IJMM.2016.08.003.
[67] C.H. Pai, H.J. Wu, C.H. Lin, A.H.J. Wang, Structure and mechanism of Escherichia coli glutathionylspermidine amidase belonging to the family of cysteine; histidine-dependent amidohydrolases/peptidases, Protein Sci. 20 (2011) 557–566, https://doi.org/10.1002/PRO.589.
[68] Z. Karaköy, E. Cadirci, B. Dincer, A new target in inflammatory diseases: lycopene, Eurasian J. Med. 54 (2022) S23–S28, https://doi.org/10.5152/EURASIANJMED.2022.22303.
[69] T. Velnar, T. Bailey, V. Smrkolj, The wound healing process: an overview of the cellular and molecular mechanisms, J. Int. Med. Res. 37 (2009) 1528–1542, https://doi.org/10.1177/147323000903700531.
[70] C. Bäuerl, G. Pérez-Martínez, F. Yan, D.B. Polk, V. Monedero, Functional analysis of the p40 and p75 proteins from Lactobacillus casei BL23, J. Mol. Microbiol. Biotechnol. 19 (2010) 231–241, https://doi.org/10.1159/000322233.